IOP Publishing Physics in Medicine and Biology

Phys. Med. Biol. **57** (2012) 517–533 doi:10.1088/0031-9155/57/2/517

A free database of radionuclide voxel S values for the dosimetry of nonuniform activity distributions

N Lanconelli[1], M Pacilio[2], S Lo Meo[1], F Botta[3], A Di Dia[3], L A Torres Aroche[4], M A Coca Pérez[4] and M Cremonesi[3]

[1] Department of Physics, Alma Mater Studiorum, University of Bologna, Viale Berti-Pichat 6/2, 40127 Bologna, Italy
[2] Department of Medical Physics, Azienda Ospedaliera S Camillo Forlanini, Piazza Forlanini 1, 00151 Rome, Italy
[3] Department of Medical Physics, European Institute of Oncology, Via Ripamonti 435, 20141 Milan, Italy
[4] Department of Medical Physics, Center for Clinical Researches, Calle 34 North 4501, Havana 11300, Cuba

E-mail: nico.lanconelli@unibo.it

Received 28 June 2011, in final form 1 November 2011
Published 4 January 2012
Online at stacks.iop.org/PMB/57/517

Abstract

The increasing availability of SPECT/CT devices with advanced technology offers the opportunity for the accurate assessment of the radiation dose to the biological target volume during radionuclide therapy. Voxel dosimetry can be performed employing direct Monte Carlo radiation transport simulations, based on both morphological and functional images of the patient. On the other hand, for voxel dosimetry calculations the voxel S value method can be considered an easier approach than patient-specific Monte Carlo simulations, ensuring a good dosimetric accuracy at least for anatomic regions which are characterized by uniform density tissue. However, this approach has been limited because of the lack of tabulated S values for different voxel dimensions and radionuclides. The aim of this work is to provide a free dataset of values which can be used for voxel dosimetry in targeted radionuclide studies. Seven different radionuclides (^{89}Sr, ^{90}Y, ^{131}I, ^{153}Sm, ^{177}Lu, ^{186}Re, ^{188}Re), and 13 different voxel sizes (2.21, 2.33, 2.4, 3, 3.59, 3.9, 4, 4.42, 4.8, 5, 6, 6.8 and 9.28 mm) are considered. Voxel S values are calculated performing simulations of monochromatic photon and electron sources in two different homogeneous tissues (soft tissue and bone) with DOSXYZnrc code, and weighting the contributions on the basis of the radionuclide emission spectra. The outcomes are validated by comparison with Monte Carlo simulations obtained with other codes (PENELOPE and MCNP4c) performing direct simulation of the radionuclide emission spectra. The differences among the different Monte Carlo codes are of the order of a few per cent when considering the source voxel and the bremsstrahlung tail, whereas the highest differences are observed at a distance close to the

 © 2012 Institute of Physics and Engineering in Medicine Printed in the UK & the USA

maximum continuous slowing down approximation range of electrons. These discrepancies would negligibly affect dosimetric assessments. The dataset of voxel S values can be freely downloaded from the website www.medphys.it.

1. Introduction

The calculation of the radiation absorbed dose is essential for evaluating risks and benefits associated with targeted radionuclide therapy (TRT) (e.g., molecular radiotherapy, radioimmunotherapy and selective internal radiotherapy). The assessment of the absorbed dose to target and non-target tissues for patient treatment planning is still a challenging issue in TRT. Methods for acquiring quantitative data on radionuclide biodistribution and for calculating the radiation absorbed dose using standard anthropomorphic models were described by the Medical Internal Radiation Dose (MIRD) committee (Loevinger *et al* 1988, Siegel *et al* 1999). These methods were originally designed to estimate average absorbed doses at the level of the organs and the whole body. Subsequently, the importance of including nonuniform activity distributions in the dosimetry evaluations has been considered, setting the basis for the dose calculation at the voxel level.

The MIRD pamphlet no. 17 (Bolch *et al* 1999) describes the principal methods to perform the voxel dosimetry: application of direct Monte Carlo radiation transport, integration of dose point kernels and the so-called voxel S value approach which follows the MIRD schema. These methods require the assessment of the three dimensional distribution of the radiopharmaceutical within the body. Over the last few years, efforts moved towards image processing methods to quantify a spatial and temporal activity distribution with good accuracy (Giap *et al* 1995, Liu *et al* 1999, Chiavassa *et al* 2006, Kramer *et al* 2011). With the advent of the latest PET/CT and SPECT/CT technologies, quantification of activity distributions can be performed with resolutions adequate for voxel dosimetry, typically of 5 mm or even less, co-registering functional and anatomic images. The information of both density pattern (CT) and cumulated activity distribution (SPECT/PET) available in a voxel geometry represents a resource that can be fully exploited by the direct Monte Carlo transport simulations, a technique able to handle tissue heterogeneities, taking into account the patient-specific anatomic geometry as well as the nonuniform source distributions (Hobbs *et al* 2009, 2011, Dewaraja *et al* 2010, Prideaux *et al* 2007). To date, the implementation of this method is very demanding and time consuming. Conversely, for anatomic regions characterized by uniform density tissue, the dose point kernel and the voxel S value techniques represent excellent options, with rapid computation and still-good dosimetric accuracy (Dieudonné *et al* 2010). In particular, the voxel S value concept is possibly the most applied, easy to implement, not requiring volume integrations of the dose point kernel over sources and targets and complying with the familiar MIRD formalism.

MIRD pamphlet No. 17 reports extensive tabulations of voxel S values, calculated with the EGS4 Monte Carlo code for some radionuclides, for three voxel dimensions (3 and 6 mm, and 0.1 mm for autoradiography applications). However, the SPECT and PET devices currently used in clinical practice offer several voxel dimensions, depending on the acquisition field of view, the reconstruction matrix, the zoom factor and the manufacturer. It is, therefore, important to have voxel S values for each clinical setting, i.e. for the given configuration of voxel geometry and dimensions. On the other hand, it is not always feasible for medical physicists working in clinical departments to perform dedicated Monte Carlo simulations to derive the needed S values.

Our aim is to provide a free dataset which can be used for voxel dosimetry in TRT studies. In this paper, a method to perform extensive calculation of voxel S values is presented. The procedures to assess accuracy are also reported. Seven different radionuclides of interest in TRT, and thirteen different voxel sizes are considered. Voxel S values are calculated by means of the EGSnrc Monte Carlo code (Kawrakow 2000), performing simulations of monochromatic photon and electron sources in two different homogeneous tissues (soft tissue and bone) and weighting the contributions on the basis of the emission spectra of the considered radionuclides. The outcomes are validated by comparison with simulations obtained with other Monte Carlo codes, such as penetration and energy loss of positrons and electrons (PENELOPE) and MCNP4c (Baró *et al* 1995, Hendricks *et al* 2000), performed independently by some of the authors.

2. Materials and methods

2.1. Monte Carlo simulations for the voxel S values database

The EGS (electron-gamma-shower) system is a general purpose package for Monte Carlo simulation of the transport of electrons and photons in an arbitrary geometry. EGS allows the simulation of particles with energies above a few keV up to several hundreds of GeV. EGSnrc implements many improvements in the physics of radiation transport, which notably increase the accuracy of the calculations, with respect to the previous version EGS4, especially at low energies (Kawrakow 2000). The voxel S values for the database were calculated with the DOSXYZnrc program. DOSXYZnrc is a software utility available within the EGSnrc package (Kawrakow and Walters 2006). Based on the EGSnrc transport code, it easily allows us to calculate the dose distributions in a cartesian voxel volume. The user can score the energy deposition in each of the designated voxels. Simulations with DOSXYZnrc were implemented by activating all the most advanced options available, such as the electron impact ionization, bound Compton scattering, photoelectron angular sampling, Rayleigh scattering and atomic relaxations.

Electron and photon transports were simulated in two different homogeneous tissues: soft tissue, having the elemental composition and physical density defined by Cristy and Eckerman (1987), and bone tissue (i.e. compact bone), as defined by ICRU Report 10b (*Physical Aspects of Irradiation* 1964). Even if the S values for both tissues are available on the website, all the data presented in this paper are related to soft tissue. Energy was scored in grids of cubic voxels, with the sources uniformly dispersed in a voxel irradiating isotropically the surrounding ones. All simulations have been carried out without using variance reduction techniques, with a cutoff energy of 1 keV for both electrons and photons. The simulated region is not an infinite medium, but regions beyond the cubical array of target voxels were also included to allow for particle backscatter. In particular, for each voxel size a region with a linear dimension five times larger than that covered by the target voxels was considered. For example, for 3 mm voxels a cubical region with side 16.5 cm was simulated, whereas the target voxels cover only a region with side 3.3 cm located at the centre of the simulated volume. In every case the source is located at the centre of the simulated volume. For each voxel size, monochromatic sources were simulated, both for photons and electrons. The energy of the photon sources was chosen according to the decay data from the Brookhaven National Laboratory database and available at www.doseinfo-radar.com (Stabin and da Luz 2002). From the same decay database, the electron spectra for the considered radionuclides were downloaded and rebinned to 10 keV bins. Figure 1 shows the beta spectra for the seven considered radionuclides. In particular, they can be separated into three different groups, according to the beta energy

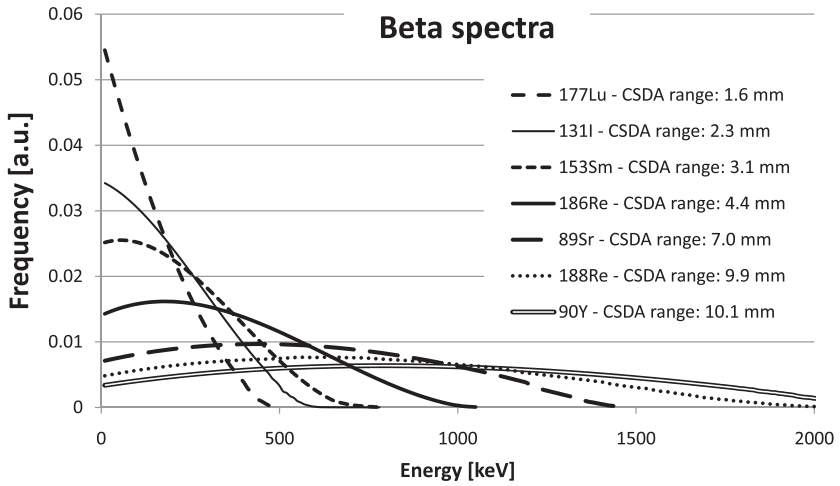

Figure 1. Beta spectra for the seven considered radionuclides. The CSDA range for the electrons with the maximum energy of each spectrum is also listed in the legend.

spectrum: low-energy radioisotopes (^{177}Lu, ^{131}I and ^{153}Sm), high-energy radioisotopes (^{188}Re and ^{90}Y) and intermediate-energy radioisotopes (^{186}Re and ^{89}Sr).

In this study, each simulation consisted in the tracking of 25 million particles (photons or electrons), with a given energy (monochromatic source), at the chosen voxel dimension. For each simulation, the energy deposited by particles in each voxel was scored. The energy was then converted in average dose to the target voxel per unit of cumulated activity (mGy MBq^{-1} s^{-1}) and associated with the target position in the cartesian grid. For each voxel size, in order to get the final S values, the contribution of all the monochromatic sources were summed, weighting by the relative abundance derived from the decay spectra. This approach allowed the calculation of voxel S values for different radionuclides, from the same ensemble of results obtained with monochromatic sources. In this way, for the voxel sizes under consideration it is also straightforward to compute the voxel S values for other radionuclides, not considered initially, without the need of performing new simulations: at this stage, only the decay spectrum of the desired radioisotope is needed to calculate the voxel S value tabulation.

2.2. Monte Carlo simulations for the quality control of the database voxel S values

In order to assess their validity, the outcomes achieved with the methods described above were compared to those obtained independently by some of the authors (co-authors MP and FB), with two other Monte Carlo codes: MCNP4c and PENELOPE. Some additional simulations were performed with EGSnrc code. The Monte Carlo calculations for quality control purposes were performed by simulating the complete beta spectrum emission for each radionuclide. Photons were simulated in a separate run and the final voxel S values were computed as the sum of photon and electron contributions.

MCNP is a general-purpose code that can be used for neutron, photon, electron or coupled neutron/photon/electron transport. It uses a three-dimensional heterogeneous geometry and can track the transport of photons and electrons in the energy range from 1 keV to about 1000 MeV. The MCNP4c code is the extended version of the originally developed MCNP code to treat also electron transport, as well as neutron and photon transport, implementing the

same algorithms as those of the ITS (integrated tiger series), version 3.0. For photon transport, the code takes into account photoelectric absorption, with the possibility of K- and L-shell fluorescent emission or Auger electron, coherent and incoherent scattering and pair production. The continuous slowing down approximation energy loss model is used for electron transport. The electron physics enhancements, including changes in the density-effect calculation for collision stopping power, radiative stopping power, calculations of bremsstrahlung spectra and angular distributions, and hard collision events, constitute the most important improvements of this code.

PENELOPE simulates coupled electron–photon transport in arbitrary materials from a few 100 eV to about 1 GeV. In this study, the 2008 version has been adopted. As regards positrons and electrons, elastic collisions are simulated using numerical partial-wave cross sections for free neutral atoms. Inelastic collisions are simulated on the basis of a generalized oscillator strength model tailored to allow fast random sampling of energy loss and recoil energy. Bremsstrahlung emission is simulated based on differential cross sections from the Seltzer and Berger database. The simulation algorithm is defined as *mixed*, separating interaction events into two different classes: *hard* events, which are simulated in detail, and *soft* events, for which condensed simulation is performed. The distinction between *hard* and *soft* events is based on the amount of energy loss and angular deflection occurring in the interaction. PENELOPE incorporates dedicated simulation control parameters adjusted by the user to fix the energy and angular thresholds separating *hard* and *soft* events. Additionally, for each material and for each particle type, the energy threshold for particle absorption (E_{abs}) can be fixed by the user, together with the maximum allowed length of the track path between two consecutive interaction events. When the particle energy drops below E_{abs}, transport is no longer simulated and residual energy is assumed to be deposited locally.

Finally, some simulations were also performed with the EGSnrc code, without using the DOSXYZnrc utility. All the parameters related to the transport of electrons and photons were the same as used for calculating the database of voxel S values.

3. Results and discussion

3.1. Results and validation

The first step of the procedure performed for getting the voxel S values for the various radionuclides consists in simulating monochromatic electron and photon sources with the DOSXYZnrc code. Figures 2 and 3 illustrate an example of some outcomes. In particular, the absorbed fraction for the self-irradiation voxel (i.e. the voxel where the source was located), calculated for monochromatic sources at different voxel sizes, is presented in figure 2. The data are reported separately for electrons and photons. For electrons, the absorbed fraction results to be very high (close to the unity) up to energy of a few hundred keV. The monotonic decreasing of the absorbed fraction with energy is due to the electron stopping power trend versus energy, whereas the increasing with voxel size reflects the increasing of the interaction probability when the voxel becomes greater. For photons, the trend versus energy is slightly more complicated. The energy range of Compton-effect dominance is very broad for low-Z media (such as human soft tissue), extending from $\approx$ 20 to $\approx$ 30 MeV, on the other hand the contribution of the photoelectric effect is still important for energies up to about 100 keV, also because the scattered photons could re-interact into the self-irradiating voxel and be absorbed by the photoelectric effect. Nevertheless, its contribution decreases rapidly, because the interaction cross section is inversely proportional to about the third power of the photon energy, as reflected by the abrupt decrease of the absorbed energy fraction. For energies higher

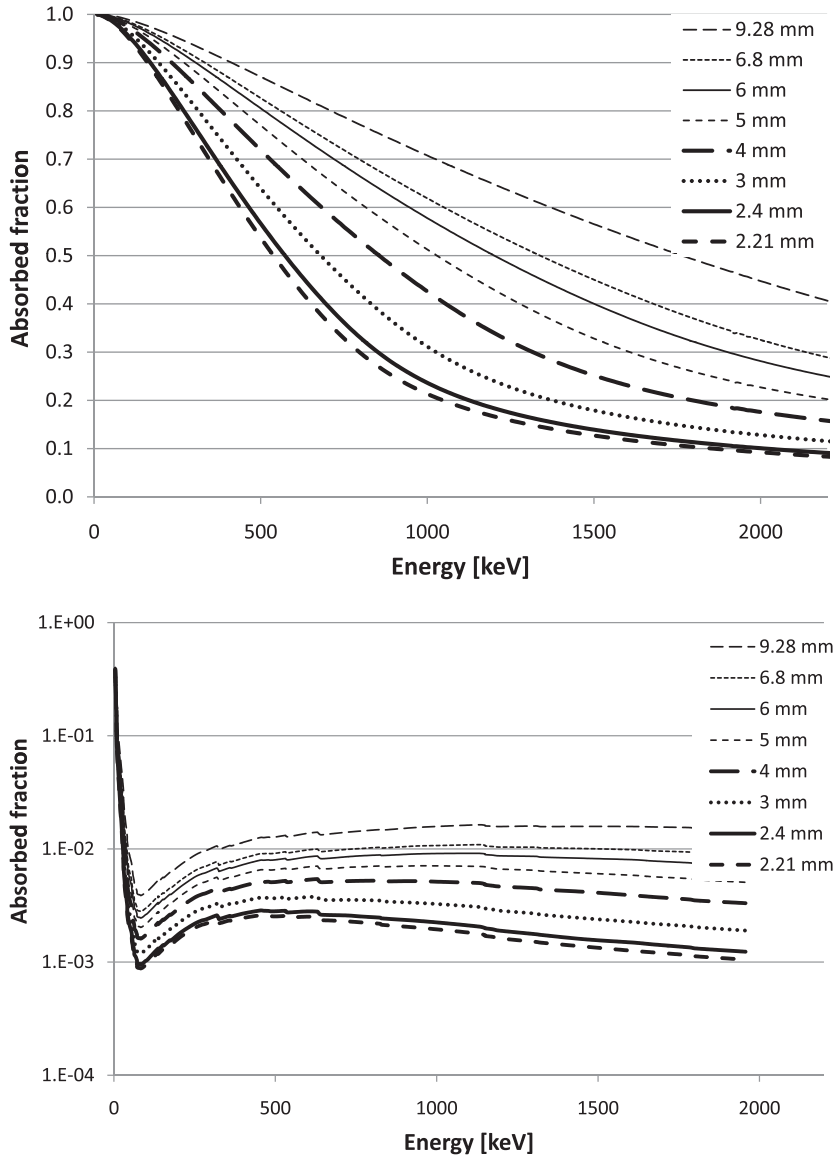

Figure 2. Absorbed fraction for the self-irradiation voxel, as a function of the energy of the source particles, calculated for monochromatic sources at different voxel sizes. Top: electron sources. Bottom: photon sources.

than about 100 keV, the absorbed energy fraction slightly increases with energy, probably due to the increase of Compton interactions with subsequent interactions of the scattered photons. For the biggest voxels, a plateau is reached at high energies, whereas for the smaller ones a subsequent lowering of the absorbed energy fraction is evidenced, due to the highest escape probability of the scattered photons when the energy increases. Correctly, as for electrons, the absorbed energy fraction increases with voxel size, as photon interaction probability increases when the voxel becomes greater. Two general trends can be observed: the absorbed fraction

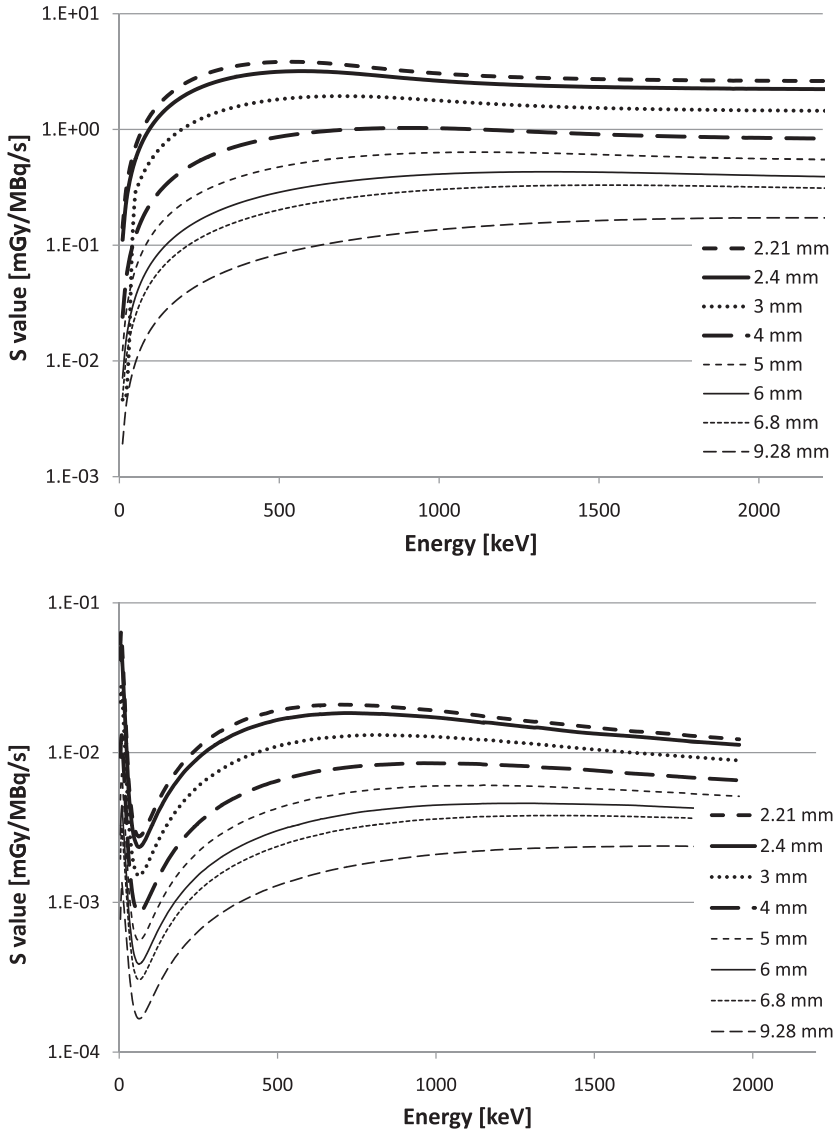

Figure 3. S values for the self-irradiation voxel, as a function of the energy of the source particles, calculated for monochromatic sources at different voxel sizes. Top: electron sources. Bottom: photon sources.

for electrons is much higher than that estimated for photons (the latter being at least a couple of orders of magnitude lower, even for low-energy photons); for both electrons and photons the absorbed fraction increases with voxel size. Figure 3 shows an example of S values for the self-irradiation voxel with monochromatic sources, as a function of the source energy, at various voxel sizes. Again, we show the data separately for electrons and photons. As the S value consists of the absorbed fraction multiplied by the energy and divided by the voxel mass, the general trends versus energy of the S values derive from the absorbed fraction trends

discussed above. As expected, in both cases S values increase as the voxel size decreases. The S values for electrons increase with energy at low energies, reaching a maximum around 600–700 keV, and finally remain constant (or slightly decrease for small voxels) at high energies, as already reported in the literature (Pacilio *et al* 2009). Similar behaviour can be observed for photons, except that they present an initial steep drop at very low energies, as discussed before.

Once a database of S values for monochromatic electrons and photons has been established for each voxel size of interest, tables of radionuclide S values may be generated. In fact, the outcomes obtained from monochromatic sources were combined to get the final voxel S values presented on the website. Figure 4 shows some results from the voxel S value database for three of the considered radionuclides (^{131}I, ^{177}Lu and ^{188}Re) and with 3 mm voxel size. S values are plotted as a function of the distance from the central voxel (self-irradiation voxel). The contribution of electrons is significant at small distances (below the maximum continuous slowing down approximation (CSDA) range), whereas photons are more important at higher distances, as expected. The tracking of electrons evidences the deposition of energy even beyond the maximum CSDA range, thanks to the bremsstrahlung photons produced during the transport. As a consequence, the curves of S values due to electrons show a sudden variation in slope at a distance close to the maximum CSDA range. From figure 4, we can note that such a distance is high for radionuclides with a high-energy beta spectrum, such as ^{188}Re. Noteworthy for this same isotope the electron contribution is about one order of magnitude higher at large distances, with respect to ^{131}I and ^{177}Lu, due to the higher energy of the emitted electrons. As expected, radionuclides with high-energy photons (e.g. ^{131}I, which has a significant abundance of 364 keV photons) present S values at large distances higher than those obtained for isotopes where photons have a lower energy (for both ^{177}Lu and ^{188}Re the photons with significant abundance have a maximum energy in the range of 100–200 keV). This behaviour is maintained for the S values calculated for the other voxel dimensions.

Figure 5 illustrates an example comparing the voxel S values from the database with those calculated by the other Monte Carlo programs (MCNP4c, PENELOPE and EGSnrc) for ^{186}Re with a voxel size of 3 mm. It can be noted from the figure that the four curves are almost indistinguishable. This happens for all the radionuclides and voxel sizes considered here, demonstrating that the outcomes of the database are in very good agreement with those obtained with some of the most common Monte Carlo codes, simulating directly the whole emission spectra of the radionuclides.

As already reported in the literature (Pacilio *et al* 2009), the statistical uncertainties associated with the voxel S values depend on the voxel size, distance between the source and target voxel, energy and type (electrons or photons) of starting particles. The overall uncertainty for the voxel S values obtained from the DOSXYZnrc monochromatic source simulations is similar to that obtained with other Monte Carlo codes. With the voxel sizes and starting particle number (25 millions) used in this work, the calculations performed with MCNP4c and PENELOPE show the following statistical uncertainties: for the self-irradiation voxel S values, always lower than about 0.02% for the beta spectrum contribution, and 0.5% for the photon emission contribution; for voxel distances in the maximum CSDA range, lower than 7%–10% for the beta contribution (for the radionuclides of lowest energy) and 2%–3% for the photon contribution; for voxel distances in the bremsstrahlung tail, lower than 20%–40% for the beta contribution and 4%–5% for the photon contribution. Considering that beyond the maximum CSDA range, the gamma contribution is at least one order of magnitude higher than that due to the bremsstrahlung photons, in that region the overall S value uncertainty is dominated by the gamma contribution.

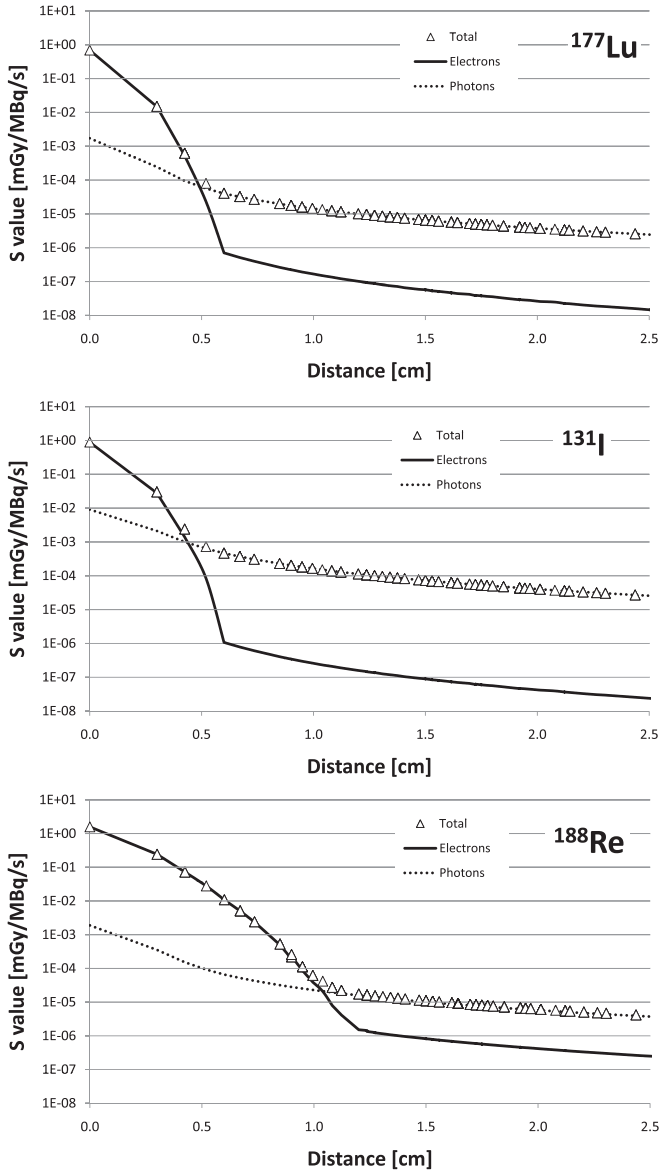

Figure 4. Voxel S values from the database, for a voxel size of 3 mm and for three different radionuclides: ^{177}Lu (top), ^{131}I (middle) and ^{188}Re (bottom). The S value contributions of photons and electrons are also reported separately.

For better analysing the data concerning the validation of the database voxel S values, in figure 6 the percentage difference of the S values calculated with the three Monte Carlo programs, with respect to those of the database, are reported for the same radionuclide and voxel size as figure 5 (^{186}Re and a voxel size of 3 mm). ^{186}Re and a voxel size of 3 mm were chosen as an example because, among all the considered radionuclides and voxel sizes, the highest differences have been observed in this case. The differences can be analysed by

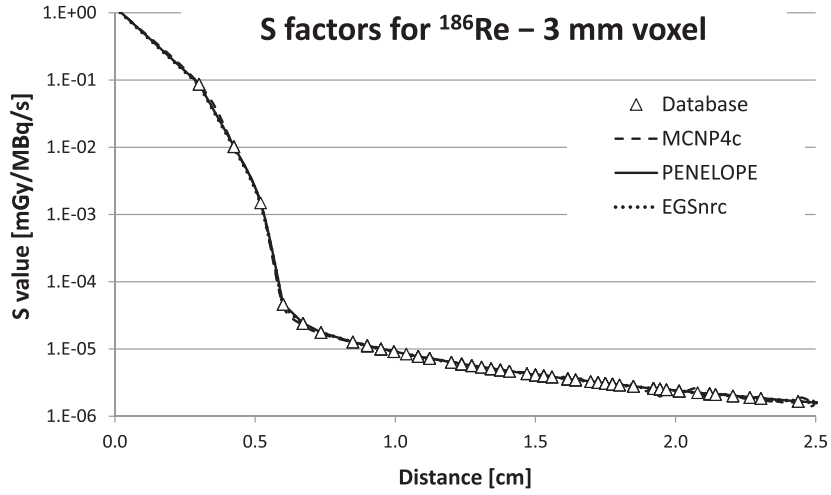

Figure 5. Comparison of voxel S values for ^{186}Re (3 mm voxel) available on our database and calculated with PENELOPE, MCNP4c and EGSnrc. The four curves are barely distinguishable, since the differences among the data are very small.

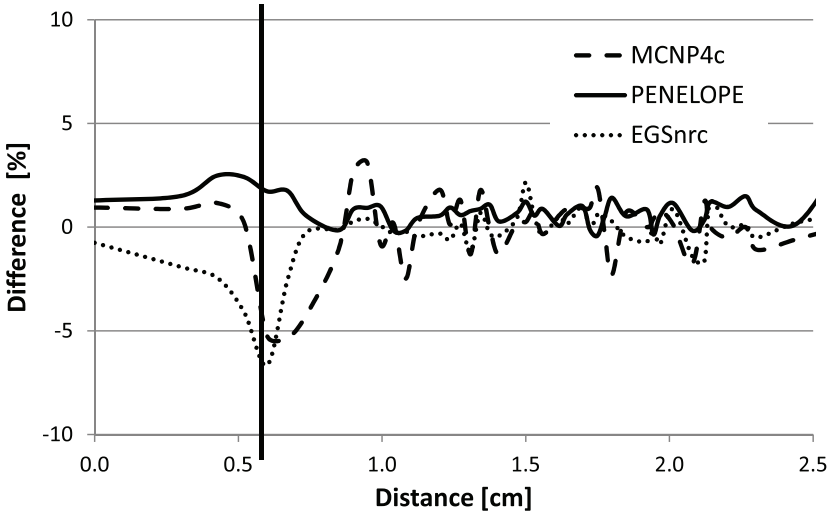

Figure 6. Percentage difference for voxel S values calculated for ^{186}Re (3 mm voxel). The differences are estimated as percentage difference, with respect to the S values of the database. The vertical line represents approximately the maximum CSDA range of electrons.

considering the entire range of distances divided into three different regions: proximity of the source (i.e. the voxel where the source is located), distances around the maximum CSDA range of electrons, reported in figure 1 ($\pm$ 1 voxel) and bremsstrahlung tail (distances greater than twice the maximum CSDA range). In all cases, for voxels in the proximity of the source the differences are within a few per cent. The highest differences occur beyond the maximum CSDA ranges. However, it is worth mentioning that at such distances the S values are several orders of magnitude lower than the self-irradiation voxel. Thus, this causes a limited overall

Table 1. Comparison of the voxel S values available in the database with those obtained with three different Monte Carlo programs (MCNP4c, PENELOPE and EGSnrc): absolute values of percentage difference, with respect to the S values of the database, are reported in three different regions, voxel where the source of radiation is located, region close to the maximum CSDA range of electrons and bremsstrahlung tail. Average behaviour among various radionuclides and voxel sizes is summarized, moreover the range of variation of percentage difference is reported in parenthesis.

	MCNP4c	PENELOPE	EGSnrc
Self-irradiation voxel	2% (1–3)	2% (0–4)	2% (1–3)
Maximum CSDA range	≈ 2% (0–5)	≈ 2% (1–5)	≈ 2% (1–5)
Bremsstrahlung tail	≈ 5% (0–15)	≈ 2% (0–10)	≈ 1% (0–2)

Table 2. Comparison of the voxel S values (mGy MBq^{-1} s^{-1}) for ^{90}Y and ^{131}I and voxel sizes of 3 mm (four rows at the top) and 6 mm (four rows at the bottom) available in the database with those published in MIRD pamphlet no 17.

(I, J, K)	Current study ^{90}Y	Bolch *et al* (1999) ^{90}Y	Current study ^{131}I	Bolch *et al* (1999) ^{131}I
(0, 0, 0)	1.59E+00	1.61E+00	8.99E-01	9.20E-01
(0, 0, 1)	2.75E-01	2.76E-01	3.02E-02	3.54E-02
(0, 1, 1)	9.50E-02	9.76E-02	2.41E-03	3.25E-03
(1, 1, 1)	4.29E-02	4.53E-02	7.26E-04	8.29E-04
(0, 0, 0)	3.42E-01	3.46E-01	1.25E-01	1.29E-01
(0, 0, 1)	3.80E-02	3.95E-02	2.47E-03	2.90E-03
(0, 1, 1)	6.86E-03	7.57E-03	2.98E-04	3.25E-04
(1, 1, 1)	1.45E-03	1.74E-03	1.63E-04	1.54E-04

impact on the dose estimation at the voxel level, as already reported by other studies (Franquiz *et al* 2003, Gonzalez *et al* 2007, Pacilio *et al* 2009, Botta *et al* 2011). The comparison was repeated for many radionuclides and voxel sizes, observing in all cases very similar behaviour: differences in the very short distance range are always within a few per cent, whereas the highest variations in terms of voxel S values take place in the proximity of the maximum CSDA range or at larger distances. In table 1, the mean difference values for each distance range are summarized.

In table 2, a comparison of some of the S values calculated in this work for ^{90}Y and ^{131}I, and the corresponding ones published in MIRD pamphlet no. 17 is summarized. The difference for the S value of the self-irradiating voxel presented here is within −1% with respect to the data from Bolch *et al* (1999) for ^{90}Y and within −2% for ^{131}I. Larger differences (down to −9% for ^{90}Y and −15% for ^{131}I) are evidenced at farther distances. A more thorough comparison was already achieved for ellipsoids (Pacilio *et al* 2009), where the authors compared voxel S values obtained by updated Monte Carlo codes, and those published in MIRD 17 (derived with the EGS4 code). In particular, a comparison for ^{90}Y and ^{131}I for two voxel sizes (3 mm and 6 mm) was reported in figures 5–8 of the previous paper, as well as a comparison of the absorbed dose for spheres and ellipsoids of various sizes (figures 11 and 12 of the same publication). In this work, differences of the same entity as the previous publication have been obtained, and this is ascribable to the differences between EGS4 and EGSnrc methods and/or cross-section libraries for transport simulation of low-energy electrons, which were also observed to affect convolution calculations producing dose differences down to −9% for ^{131}I (Pacilio *et al* 2009). The influence of the differences among updated Monte Carlo codes was also studied: it appeared much more mitigated (within a few per cent), leading to the conclusion that either one of the currently available general purpose Monte Carlo programs is

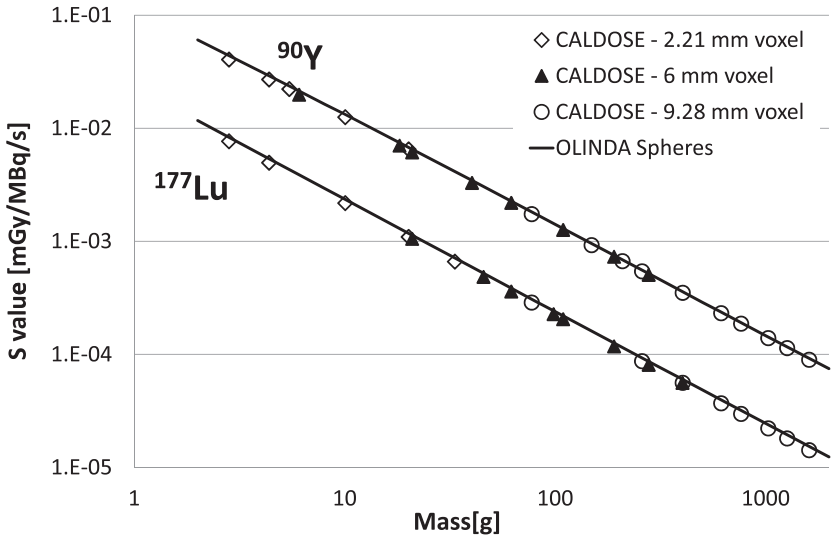

Figure 7. Mean doses for spheroidal cluster of voxels, calculated with CALDOSE and the voxel S values from the website (voxel sizes of 2.21, 6 and 9.28 mm), and for spheres of the same masses, derived from the values used in the OLINDA/EXM software, for ^{177}Lu and ^{90}Y.

suitable to produce voxel S values for TRT (Pacilio *et al* 2009). The Monte Carlo simulations performed in this work for achieving the quality control of the database showed that the data in the website are perfectly in-line with the results derived with updated general purpose Monte Carlo codes.

For further validation, mean doses absorbed to spheroidal cluster of voxels were calculated using the kernels in the database for different voxel sizes, and compared with mean absorbed doses for spherical masses quoted in the RADAR website (www.doseinfo-radar.com) and used in the OLINDA/EXM software (Stabin *et al* 2005). The JAVA software program named CALDOSE (calculations of dose on spheres and ellipsoids) previously developed by the authors (Pacilio *et al* 2009) was used for dose convolution calculations. To assess the range of difference based on one-by-one comparisons, the mean doses for sphere masses equal to the cluster ones were obtained by fitting the OLINDA data with an inverse power law. As an example, such a comparison is reported in figure 7 for ^{177}Lu and ^{90}Y, the least and the most energetic beta emitters among those studied here, referring to voxel sizes of 2.21, 6 and 9.28 mm. With masses in the range 2–1600 g, the differences with respect to the OLINDA mean absorbed doses ranged from −7.7% to −6.3% for ^{177}Lu and from −7.9% to −2.1% for ^{90}Y. As the mean doses of OLINDA sphere masses have been calculated with the older MCNP4B and EGS4 codes (Stabin and Konijnenberg 2000), these differences appear in agreement with the results discussed above, even though the density difference between the unit density spheres of OLINDA and the soft tissue density employed here (i.e. 1.04 g cm^{-3}) can also play a role. Indeed, calculating with MCNP4c the voxel S values associated with position indices of (0, 0, 0), (0, 0, 1), (0, 1, 1) and (1, 1, 1) for the two density values, the following differences were observed: from 6.9% to 3.3% (for self-irradiating voxel) for ^{177}Lu, and from 5.7% to 0.5% (for self-irradiating voxel) for ^{90}Y. This is in quite good agreement with the trend of the observed mean dose differences. Similar results were obtained for the other radionuclides studied here.

3.2. Dataset available in the website

At present, the database consists of 7 radionuclides (^{89}Sr, ^{90}Y, ^{131}I, ^{153}Sm, ^{177}Lu, ^{186}Re and ^{188}Re) and cubic voxels with 13 different sides (2.21, 2.33, 2.4, 3, 3.59, 3.9, 4, 4.42, 4.8, 5, 6, 6.8 and 9.28 mm). For each radionuclide and voxel dimension, the plot of S values is displayed as a function of the distance from the source voxel. This allows the user to have a quick look at the general trend of the S values. In addition, users can download the entire list of voxel S values (photon and electron contributions) as a text file. Such data are the ones needed to calculate the dose distribution as a convolution between the S values matrix and the cumulated activity map. Following the MIRD pamphlet no. 17 (Bolch *et al* 1999), data are provided as a function of voxel cartesian coordinates starting from (0, 0, 0), representing the source voxel, up to position indices of (5, 5, 5). For each condition, the voxel S value is indexed to the integer coordinates of the target voxel in all dimensions (I, J, K). Each entry (I, J, K) indicates values for the voxel located at a distance from the source voxel of I voxels in the first dimension, J voxels in the second and K voxels in the third dimension, respectively. The isotopes and voxel sizes considered up to now were chosen among the most widespread radioisotopes for TRT and the most common voxel sizes found in clinical SPECT/CT systems. However, thanks to the methodology used for the calculation, it is quite effortless to calculate the S values for other radionuclides. The site is also open to possible requests from the users having different needs, for example, other voxel sizes, including PET devices, and accounting not only for the nominal but also the real resolution of the system.

3.3. Recommendations on using website data and obtaining new data from those actually available

The accuracy of the data reported in the website was extensively checked, so these datasets may constitute a useful datum point, preventing less experienced users from possible mistakes in using Monte Carlo codes. On the other hand, the use of voxel S values from pre-calculated datasets presents some intrinsic limitations. It is not possible to derive, from the website, data for non-cubical voxels or for radionuclides and/or for media different from those explicitly covered, without achieving accuracy limitations of unpredictable extent. Conversely, alternative calculation strategies of voxel S values should be more versatile for taking into account possible voxel size/geometry variations (Franquiz *et al* 2003, Sarfaraz *et al* 2004, Dieudonné *et al* 2010).

The users are also strongly advised not to extend the validity of these data to different media, or to physical or clinical conditions unconformable with the hypothesis of uniform tissue density and composition, in particular, if disease or other conditions may cause significant deviations from the calculation assumptions. Unfortunately, due to the non-linear nature of dose deposition, not even linear interpolation for cubical voxels of different size is advisable, even though a strategy to strongly reduce interpolation errors can be afforded. Converting S values into absorbed energy could minimize these errors, as the term containing the voxel mass is intrinsically non linear with voxel size. In figures 8 and 9 examples of the errors resulting from linear interpolation are reported for ^{90}Y and ^{177}Lu, respectively. Data are referred to voxel sizes of 2.40, 3.59 and 6 mm, whose corresponding S values were first interpolated and after compared with those provided in the website. The interpolation procedure was done either with voxel S values or with the corresponding values of deposited energy (E_{dep}). It can be noticed that the percentage differences between interpolated and provided values are strongly reduced when interpolation is based on E_{dep} datasets.

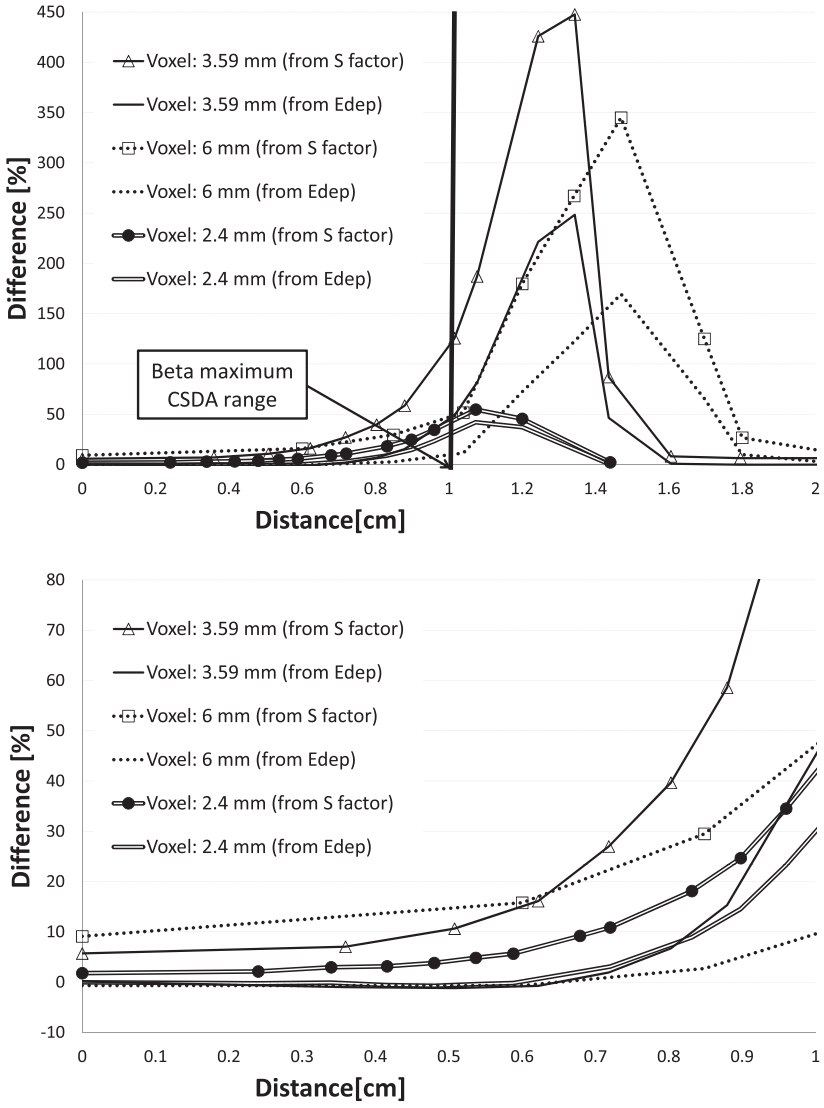

Figure 8. Errors resulting from linear interpolation for ^{90}Y for three different voxel sizes. The difference is calculated between the values provided in the website and the same values interpolated from the two closest available voxel sizes. The interpolation procedure was done either with voxel S values (namely, from S factor), or with the corresponding values of deposited energy (namely, from E_{dep}). Top: full range of distances. Bottom: zoom of the plot at small distances.

3.4. 3D dosimetry using S-voxel values in clinical application: possible advantages and drawbacks

The importance of dose calculation at the voxel level is related to the possibility of considering the inherent heterogeneity of the radiopharmaceutical distribution in tumour and normal organs, and the different tissue density and composition as well. Several clinical studies have shown that the inclusion of nonuniform activity distributions in the dosimetry evaluations is able to provide more detailed information regarding the potential efficacy and toxicity

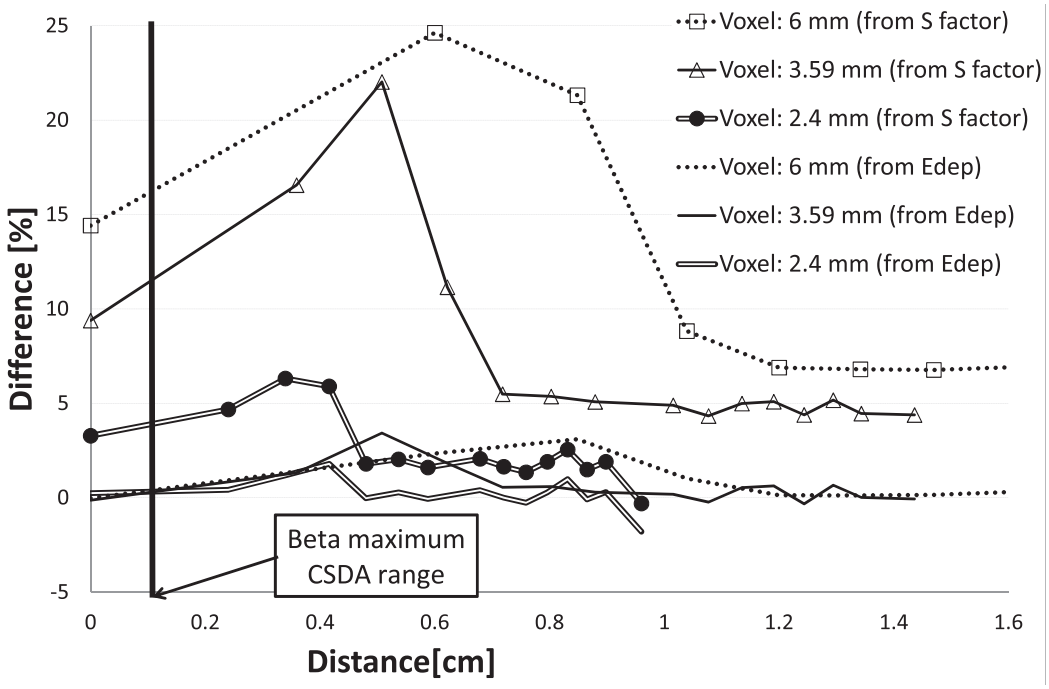

Figure 9. Errors resulting from linear interpolation for ^{177}Lu for three different voxel sizes. The difference is calculated between the values provided in the website and the same values interpolated from the two closest available voxel sizes. The interpolation procedure was done either with voxel S values (namely, from S factor) or with the corresponding values of deposited energy (namely, from E_{dep}).

(Hobbs *et al* 2009, 2011, Dewaraja *et al* 2010, Prideaux *et al* 2007). The dose distribution data allow the calculation of radiobiological parameters that take into account the nonuniformity of the dose distribution and correlate with the biological effect better than other dosimetric parameters, such as the average dose (Dewaraja *et al* 2010). A high degree of heterogeneity has been evidenced in both tumours and normal organs, with maximum doses more than twice the average dose. In particular, in tumours mean absorbed doses even tenfold higher than the equivalent uniform doses were observed (Hobbs *et al* 2009, Prideaux *et al* 2007). The inclusion of nonuniformity impacted favourably on the treatment planning, enhancing the chance of response, thanks to the substantial increase of the administered activity (e.g., 2.6-fold, (Hobbs *et al* 2009)) with no toxicity developed. Moreover, in the case of treatments combining radiopharmaceutical therapy and external beam radiotherapy, the availability of dose maps of both treatments is particularly useful to derive cumulative dose volume histograms and properly tailor each step of the treatment (Hobbs *et al* 2011).

All these studies prove that 3D voxel dosimetry is more suitable for optimizing the single patient risk–benefit balance and, in general, for deriving more robust dose–effect correlations for both tumours and normal tissues. Although they all adopted a direct Monte Carlo simulation method, all the advantages above reported are typical of 3D dosimetry approach, so they still apply to the S-voxel dosimetry as long as the hypothesis of homogeneous tissue composition is reliable (Dieudonné *et al* 2010). Specific S-voxel values for particular densities such as bone or lung must be used to evaluate the absorbed dose in these tissues, but the S-voxel method

cannot be applied in the case of interface. In fact, errors would arise depending on specific scenarios including radionuclides, geometry, density gradient and activity distribution. In such cases, the use of direct MC simulations is certainly recommended instead. The dosimetric impact of density heterogeneity in the case of different TRTs, critical organs and tumour sites is a matter of interest, together with the problems related to the degradation of the images (Ljungberg *et al* 2003). These issues are an object of study by many groups, including ours.

4. Summary

In this paper a website is presented containing an accurate dataset of voxel S values to be used for voxel dosimetry calculation in TRT studies. Data can be freely downloaded at the website www.medphys.it. Seven different radionuclides of interest in TRT, and thirteen different voxel sizes for largely widespread imaging systems were considered. The DOSXYZnrc Monte Carlo program was used to simulate S values for monoenergetic sources of photons and electrons, subsequently combined according to the emission spectra to obtain isotopes S values. The accuracy of the procedure to achieve the data included in the website was assessed by comparison with the outcomes of two other Monte Carlo codes (MCNP4c, PENELOPE), obtained simulating the entire emission spectrum in a single simulation run. The differences among the codes are of the order of a few percent close to the source voxel and in the bremsstrahlung tail. The highest discrepancies occur at a distance close to the maximum range of electrons, where, however, S values are at least three orders of magnitude lower than those of the source voxel, thus leading to minor impact on the dose estimation at the voxel level.

References

Baró J, Sempau J, Fernández-Varea J M and Salvat F 1995 PENELOPE: an algorithm for Monte Carlo simulation of the penetration and energy loss of electrons and positrons in matter *Nucl. Instrum. Methods Phys. Res.* B **100** 31–46

Bolch W E *et al* 1999 MIRD pamphlet No. 17: the dosimetry of nonuniform activity distributions-radionuclide S values at the voxel level *J. Nucl. Med.* **40** 11S–36S

Botta F *et al* 2011 Calculation of electron and isotopes dose point kernels with FLUKA Monte Carlo code for dosimetry in nuclear medicine therapy *Med. Phys.* **38** 3944–54

Chiavassa S, Aubineau-Lanice I, Bitar A, Lisbona A, Barbet J, Franck D, Jourdain J R and Bardis M 2006 Validation of a personalized dosimetric evaluation tool (Oedipe) for targeted radiotherapy based on the Monte Carlo MCNPX code *Phys. Med. Biol.* **51** 601–16

Cristy M and Eckerman K F 1987 Specific absorbed fractions of energy at various ages from internal photon sources *Technical Report* ORNL/TM-8381/V1, Oak Ridge National Laboratory, TN, USA

Dewaraja Y K, Schipper M J, Roberson P L, Wilderman S J, Amro H, Regan D D, Koral K F, Kaminski M S and Avram A M 2010 131I-Tositumomab radioimmunotherapy: initial tumor dose response results using 3-dimensional dosimetry including radiobiologic modeling *J. Nucl. Med.* **51** 1155–62

Dieudonné A, Hobbs R F, Bolch W E, Sgouros G and Gardin I 2010 Fine-resolution voxel S values for constructing absorbed dose distributions at variable voxel size *J. Nucl. Med.* **51** 1600–7

Franquiz J M, Chigurupati S and Kandagatla K 2003 Beta voxel S values for internal emitter dosimetry *Med. Phys.* **30** 1030–2

Giap H B, Macey D J and Podoloff D A 1995 Development of a SPECT-based three-dimensional treatment planning system for radioimmunotherapy *J. Nucl. Med.* **36** 1885–94

Gonzalez J, Calderón C and Rodriguez M 2007 Determination of radionuclide 'S' values for any voxel size, based on three-dimensional discrete Fourier transform convolution method world *J. Nucl. Med.* **6** 40–4

Hendricks J S, Adams K J, Booth T E, Briesmeister J F, Carter L L, Cox L J, Favorite J A, Forster R A, McKinney G W and Prael R E 2000 Present and future capabilities of MCNP *Appl. Radiat. Isot.* **53** 857–61

Hobbs R F, McNutt T, Baechler S, He B, Esaias C E, Frey E C, Loeb D M, Wahl R L, Shokek O and Sgouros G 2011 A treatment planning method for sequentially combining radiopharmaceutical therapy and external radiation therapy *Int. J. Radiat. Oncol. Biol. Phys.* **80** 1256–62

Hobbs R F, Wahl R L, Lodge M A, Javadi M S, Cho S Y, Chien D T, Ewertz M E, Esaias C E, Ladenson P W and Sgouros G 2009 124I PET-based 3D-RD dosimetry for a pediatric thyroid cancer patient: real-time treatment planning and methodologic comparison *J. Nucl. Med.* **50** 1844–7

Kawrakow I 2000 Accurate condensed history Monte Carlo simulation of electron transport. I. EGSnrc, the new EGS4 version *Med. Phys.* **27** 485–98

Kawrakow I and Walters B R B 2006 Efficient photon beam dose calculations using DOSXYZnrc with BEAMnrc *Med. Phys.* **33** 3046–56

Kramer R, Richardson R B, Cassola V F, Vieira J W, Khoury H J, de O Lira C A B and Brown K R 2011 Electron absorbed fractions of energy and S-values in an adult human skeleton based on μCT images of trabecular bone *Phys. Med. Biol.* **56** 1803–36

Liu A, Williams L E, Lopatin G, Yamauchi D M, Wong J Y and Raubitschek A A 1999 A radionuclide therapy treatment planning and dose estimation system *J. Nucl. Med.* **40** 1151–3

Ljungberg M, Frey E, Sjögreen K, Liu X, Dewaraja Y and Strand S 2003 3D absorbed dose calculations based on SPECT: evaluation for 111-In/90-Y therapy using Monte Carlo simulations *Cancer Biother. Radiopharm.* **18** 99–107

Loevinger R, Budinger T F and Watson E E 1988 *MIRD Primer for Absorbed Dose Calculations* (New York: Society of Nuclear Medicine)

Pacilio M, Lanconelli N, Lo Meo S, Betti M, Montani L, Aroche L A T and Perez M A C 2009 Differences among Monte Carlo codes in the calculations of voxel S values for radionuclide targeted therapy and analysis of their impact on absorbed dose evaluations *Med. Phys.* **36** 1543–52

Physical Aspects of Irradiation 1964 *ICRU Report* 10 b *(National Bureau of Standards Handbook* 85*)* (Bethesda, MD: National Bureau of Standards)

Prideaux A R, Song H, Hobbs R F, He B, Frey E C, Ladenson P W, Wahl R L and Sgouros G 2007 Three-dimensional radiobiologic dosimetry: application of radiobiologic modeling to patient-specific 3-dimensional imaging based internal dosimetry *J. Nucl. Med.* **48** 1008–16

Sarfaraz M, Kennedy A S, Lodge M A, Li X A, Wu X and Yu C X 2004 Radiation absorbed dose distribution in a patient treated with yttrium-90 microspheres for hepatocellular carcinoma *Med. Phys.* **31** 2449–53

Siegel J A *et al* 1999 MIRD Pamphlet No. 16: Techniques for quantitative radiopharmaceutical biodistribution data acquisition and analysis for use in human radiation dose estimates *J. Nucl. Med.* **40** 37S–61S

Stabin M and da Luz L 2002 Decay data for internal and external dose assessment *Health Phys.* **83** 471–5

Stabin M G, Sparks R B and Crowe E 2005 OLINDA/EXM: the second-generation personal computer software for internal dose assessment in nuclear medicine *J. Nucl. Med.* **46** 1023–7

Stabin M and Konijnenberg M 2000 Re-evaluation of absorbed fractions for photons and electrons in spheres of various sizes *J. Nucl. Med.* **41** 149–60